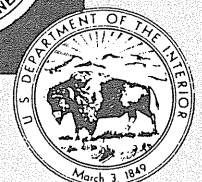


# Rapid (Grab) Sampling During Full-Scale Explosions—Microscopic and Analytical Evaluation

By Ronald S. Conti, Isaac A. Zlochower,  
and Michael J. Sapko

BUREAU OF MINES

UNITED STATES DEPARTMENT OF THE INTERIOR



**Report of Investigations 9192**

**Rapid (Grab) Sampling During Full-Scale  
Explosions—Microscopic and Analytical  
Evaluation**

**By Ronald S. Conti, Isaac A. Zlochower,  
and Michael J. Sapko**

**UNITED STATES DEPARTMENT OF THE INTERIOR  
Donald Paul Hodel, Secretary**

**BUREAU OF MINES  
T S Ary, Director**

**Library of Congress Cataloging in Publication Data:**

**Conti, Ronald S.**

Rapid (grab) sampling during full-scale explosions.

(Bureau of Mines Report of investigations; 9192)

Bibliography: p. 16

Supt. of Docs. no.: I 28.23:9192.

1. Mine explosions. 2. Mine gases--Measurement.  
I. Zlochower, Isaac A. II. Sapko, M. J. III. Title. IV. Series: Report of  
investigations (United States. Bureau of Mines); 9192.

TN23.U43

[TN306]

622 s [622'.8]

88-14520

## CONTENTS

	<i>Page</i>
Abstract .....	1
Introduction .....	2
Acknowledgments .....	2
Sampling system .....	2
Trigger mechanism .....	4
Scanning electron microscope studies .....	5
Lake Lynn experimental mine .....	8
LLEM test 110 .....	10
LLEM test 111 .....	12
LLEM test 112 .....	13
Gas analyses .....	14
Thermodynamic calculations .....	15
Conclusion .....	16
References .....	16
Appendix.-List of symbols .....	18

## ILLUSTRATIONS

1. Perspective view of mine-scale version of rapid-sampling system mechanism .....	2
2. Cross-sectional view of rapid-sampling device, in quiescent and activated states .....	3
3. Perspective view of triggering mechanism .....	4
4. Electrical schematic of triggering circuit .....	5
5. Typical SEM photomicrographs of burned and unburned Pittsburgh coal and 65% rock dust particles. .	6
6. X-ray spectra of Pittsburgh coal and rock dusts .....	7
7. Illustration of typical sampling cycle with respect to flame arrival and to trailing edge of flame for three Lake Lynn experiments .....	7
8. Plan view of Lake Lynn underground mine .....	8
9. Plan view of face area in D drift showing configuration of nominal dust loading for a single entry . . . .	8
10. Wave diagram of single-entry coal dust 65% rock dust explosion LLEM test 110 D drift .....	9
11. Complete sampling system installed in D drift .....	10
12. Photomicrographs of dust collected with sampling device during LLEM 110 explosion test in D drift . .	11
13. Photomicrograph of large residue collected with sampling system .....	13
14. Photomicrographs of partially devolatilized coal particles, sampled before and during the explosion . . .	13
15. Photomicrograph of partially devolatilized coal particle .....	14

## TABLES

1. Performance of sampling system .....	12
2. Actual burned gas compositions from LLEM tests 110, 111, 112, with corresponding flame arrival times .....	12
3. Average dry gas composition .....	15

## UNIT OF MEASURE ABBREVIATIONS USED IN THIS REPORT

atm	atmosphere	m <sup>3</sup>	cubic meter
cal	Calorie	mg	milligram
cm	centimeter	mg/ms	milligram per millisecond
cm <sup>3</sup>	cubic centimeter	mm	millimeter
ft	foot	ms	millisecond
g	gram	ppm	part per million
g/m <sup>3</sup>	gram per cubic meter	psi	pound per square inch
K	kelvin	psig	pound per square inch, gauge
keV	kilo electron volt	s	second
kg	kilogram	μm	micrometer
kΩ	kilohm	Vac	volt, alternating current
L	liter	Vdc	volt, direct current
m	meter	vol %	volume percent
m/s	meter per second	W/cm <sup>2</sup>	watt per square centimeter
m <sup>2</sup>	square meter		

# RAPID (GRAB) SAMPLING DURING FULL-SCALE EXPLOSIONS—MICROSCOPIC AND ANALYTICAL EVALUATION

By Ronald S. Conti,<sup>1</sup> Isaac A. Zlochower,<sup>2</sup> and Michael J. Sapko<sup>3</sup>

---

## ABSTRACT

The Bureau of Mines has developed a system using a high-speed electropneumatic mechanism for the rapid (grab) sampling of dusts and gases during an explosion. The sampling system consists of an aluminum housing that incorporates two 30-cm<sup>3</sup> preevacuated glass vials with rubber septums. Upon actuation, the sampling probe needle is driven through the septum with a pressurized air pulse, filling the tube with gas and dust from the mine explosion. After a predetermined time, the sampling probe needle is retracted by a second high-pressure air pulse to its normal (quiescent) state, allowing the sampling tube to reseal. The onset and the duration of sampling are independently variable and controlled by a time-delay relay package. This technique enables the monitoring of pyrolysis-charring in coal particles and the generation and combustion of the pyrolysis vapors in both large- and small-scale explosions. The following results were obtained from full-scale dust explosion tests at the Bureau of Mines Lake Lynn Laboratory: (1) Gas sampling of the leading edge of the flame front shows the large concentration changes, characteristic of the flame front; (2) gas samples taken entirely in the flame zone consist of pyrolysis and combustion products with very low residual oxygen; and (3) the particles collected in the flame zone show signs of extensive pyrolysis and charring.

---

<sup>1</sup>Electronics engineer.

<sup>2</sup>Research chemist.

<sup>3</sup>Supervisory chemical engineer.

Pittsburgh Research Center, Bureau of Mines, Pittsburgh, PA.

## INTRODUCTION

Coal dust explosion research has been conducted for many years by the Bureau to gain an understanding of the requirements of ignition, propagation, and inhibition of dust explosions. Considerable technical and practical information has been gained from this research, which was used in establishing the present safety standards in the mining industry. Nonetheless, dust explosion studies in experimental mines continue to be predominantly empirical because of the absence of a detailed theoretical understanding of the initiation and propagation of combustion waves in mine configurations. Much of the

difficulty in developing a theoretical basis is associated with the limitation of the experimental techniques for studying the chemical aspects of full-scale mine gas and dust explosion processes. This report describes a rapid (grab) sampling system for collecting small samples of dusts and gases from the rapidly moving (90 to 300 m/s) flame front and hot gas zone. This sampling system should promote the collection of accurate chemical data to expand the knowledge of the flammability behavior of dusts, gases, and inhibitors, which is essential for the realistic appraisal of the explosion hazards involved in coal mining.

## ACKNOWLEDGMENTS

The authors wish to thank the important contributions of the following members of the Bureau's Pittsburgh (PA) Research Center: J. Leong, electronics technician, for his initial assistance in the preparation of the sampling system; R. Pro and G. Green, physical science technicians, for

their assistance with the installation of the sampling system at the Lake Lynn experimental mine (LLEM); and R. Thomas, engineering technician, for his assistance in data collection.

## SAMPLING SYSTEM

The mechanical device used to obtain rapid gas and dust grab samples is shown in a sectional perspective in figure 1. The main components of the system are an electropneumatic, double-acting air cylinder (Bimba Manufacturing Co.)<sup>4</sup> to power the sampling system, a piston section to which the sampling probe needles are attached, and the housing for the evacuated (glass) collection tubes. A time-delay relay package controls a high-pressure air solenoid valve that directs the air pulses to the double-acting air cylinder.

The sampling system is shown in more detail in figure 2. The main body is essentially a rectangular aluminum housing with two cylindrical holes that contain the 30-cm<sup>3</sup> glass collection tubes. To guard against the mechanical shock caused by the forward thrust of the sampling probe needles, rubber inserts are fitted into the bottom of each hole to serve as shock absorbers for the collection tubes. The center portion of the main body (back side) is milled parallel to the collection tubes, to provide mounting space for the double-acting air cylinder. The housing cover serves a threefold purpose, it allows access to the collection tubes, holds the sealed collection tubes in place, and serves as a guide for the sampling probe needles.

The two sampling probe needles are mounted on a support bar, which is attached to the piston rod of the double-acting air cylinder. The sampling probe needle is a modified 11-gauge, hypodermic needle (stainless steel). The beveled point of the needle is plugged and then silver soldered, and a 1.6-mm-diam hole is drilled through

the side close to the point. This modification minimizes the risk of septum tearing or core boring by the needle penetration, thereby allowing the septum to reseal (reducing leakage of the collection tube) during the return cycle of the air cylinder.

When the system is in the activated state (fig. 2), the combustion products are drawn into the evacuated collection tube. When the preset sampling time is reached, the probe needle returns to its initial position or quiescent state, allowing the rubber septum of the collection tube to reseal. This predetermined sampling time is controlled by a series of time-delay relays that send electrical pulses to a high-speed, direct-solenoid actuated

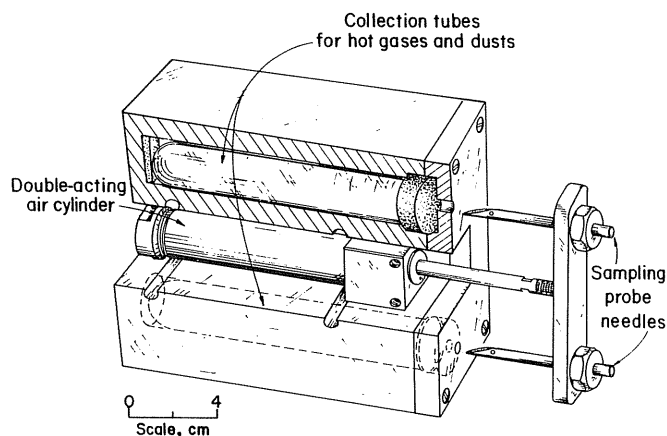


Figure 1. - Perspective view of mine-scale version of rapid-sampling system mechanism.

<sup>4</sup>Reference to specific products does not imply endorsement by the Bureau of Mines.

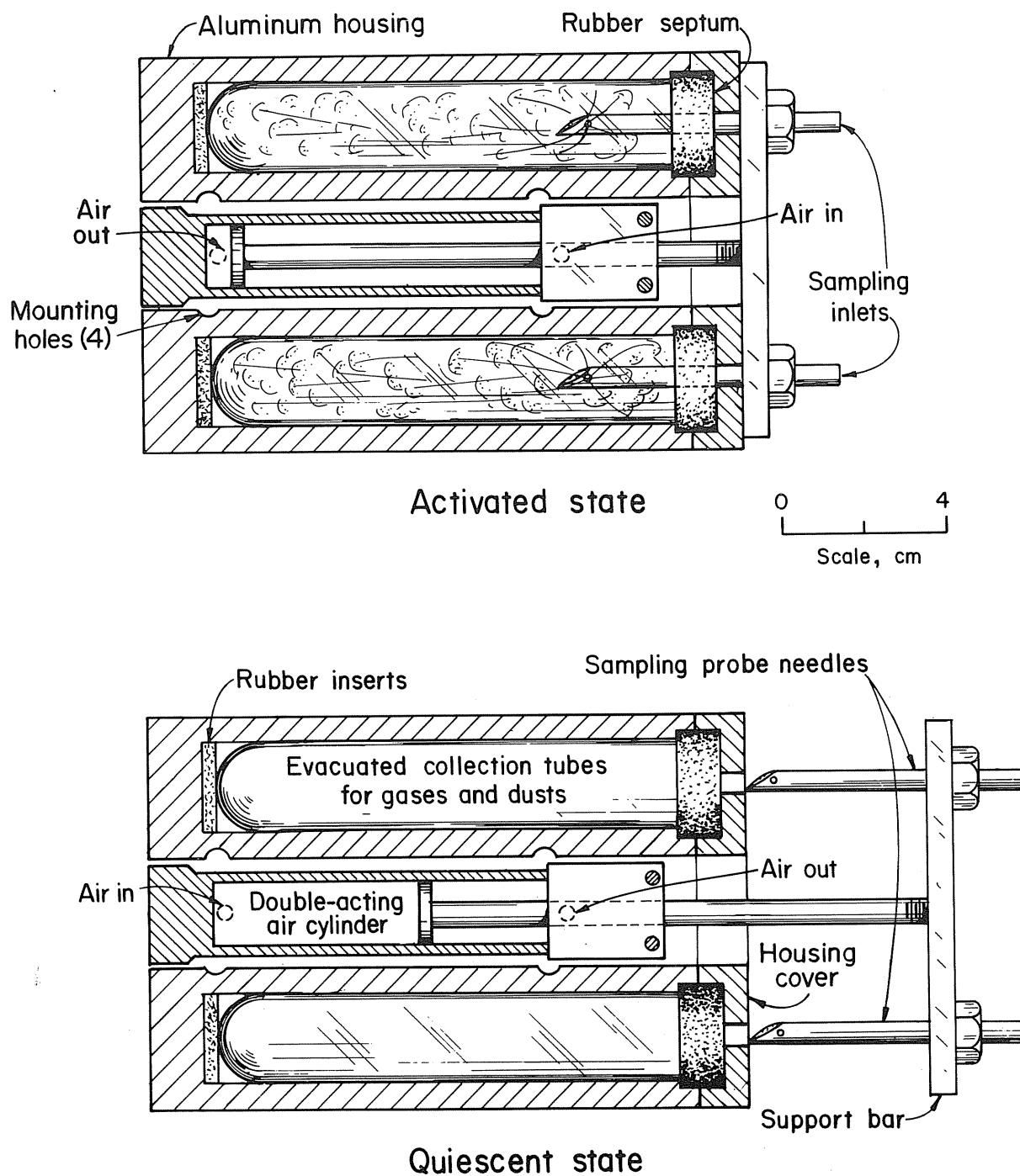


Figure 2. - Cross-sectional view of rapid-sampling device, in quiescent and activated states.



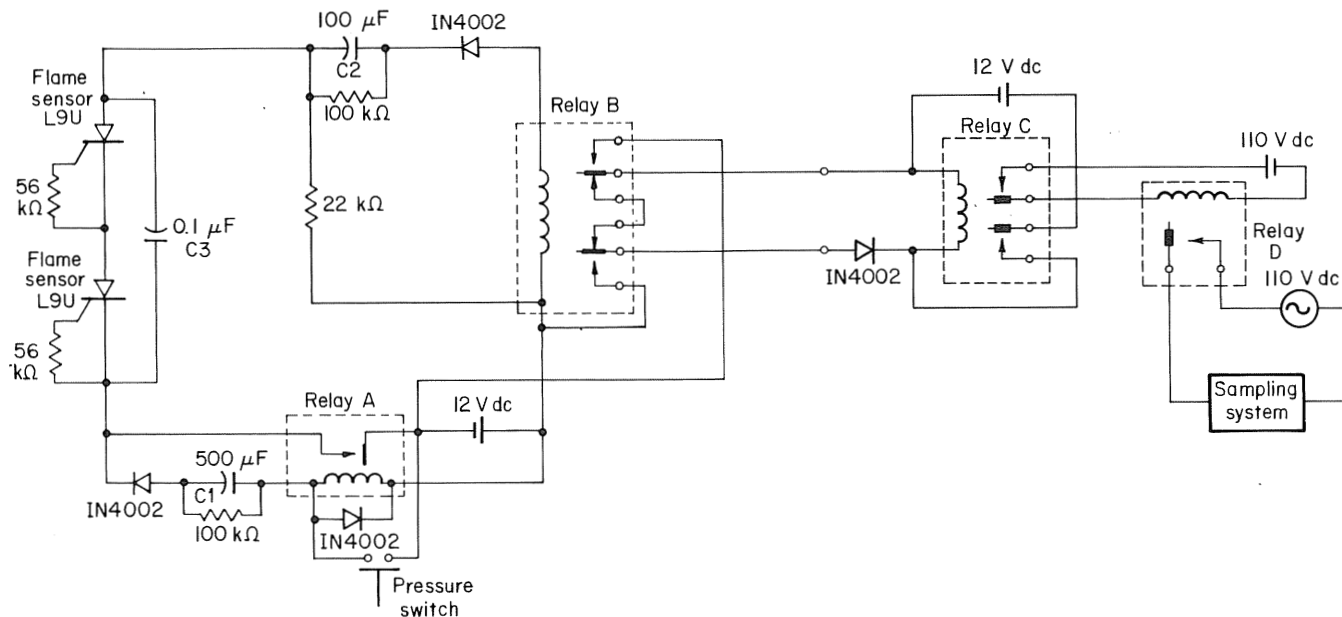


Figure 4. - Electrical schematic of triggering circuit.

## SCANNING ELECTRON MICROSCOPE STUDIES

The microscopic structure of coal dust-rock dust mixtures was analyzed by a scanning electron microscope (SEM) system. A detailed description of the SEM, and fire and explosion residues for various dusts can be found in reference 6. A typical photomicrograph of a 65% rock dust ( $\text{CaCO}_3$ ) Pittsburgh pulverized coal mixture, both burned and unburned is shown in figure 5. The unburned coal particles (fig. 5A) collected prior to the explosion have distinct characteristics, sharp edges and angular features, as opposed to the smooth rounded edges of the burned coal particles shown in figure 5B, which were collected during flame passage of one of the experiments (LLEM 110).

Figure 6 compares the X-ray spectra of rock dust (fig. 6A) with those of coal dust (6B). Notice the strong calcium lines,  $\text{K}\alpha$  at 3.7 keV and  $\text{K}\beta$  at 4.01 keV. The other elements shown reflect the copper sample substrate,

interface media of sample, and the gold and platinum coating of the sample. A collection of all the calcium X-ray photons produced during the electron beam scanning of the samples shown in figures 5A and 5B were used to make the X-ray elemental maps in figures 5C and 5D, respectively. The maps can be used to identify the rock dust particles and how they interact with the coal particles before and after flame passage.

A sampling cycle representing six sampling stations is shown in figure 7. The pulses shown for three tests, 110, 111, and 112, illustrate when the sampling device is activated and when the device returns to its quiescent state. The shaded portion represents the radiation zone, from flame arrival to trailing edge of flame. The numbers at the top of each cycle boundary indicate the distance between the sampling station and the leading edge of the flame.

valve. The initial pulse directs high-pressure (150 psi) air or N<sub>2</sub> from the solenoid valve to a port of the double-acting air cylinder, which forces the sampling probe needles forward into the collection tubes (the activated state). A similar pulse applied to the opposite port of the double-acting air cylinder returns the sampling probe assembly to its quiescent state, thus completing the sample cycle.

After the experiments, the sampling probe needles are removed from the support bar to be cleaned in an ultrasonic bath. The housing cover is unfastened and the collection tubes are removed for a complete analysis. The contents of one collection tube is used for gas analysis and the other, typically, for microscopic analysis of the dust residue. This mine-scale version of the rapid sampling system is similar in concept to the previously

reported laboratory version (1)<sup>5</sup> in the utilization of the double-acting air cylinders, the glass collection tubes, and the sampling probe needles. The main difference between the two systems is essentially in the operation of the sampling probe needles. In the laboratory version, the sampling probe needles are stationary (fastened to the test apparatus) and the glass collection tube moves with the piston. It was especially designed to interface with the Bureau's ignitability furnace (2). The timing of the sequences in the laboratory version is controlled by a microprocessor. A detailed description can be found in reference 1.

<sup>5</sup>Italic numbers in parentheses refer to items in the list of references preceding the appendix.

## TRIGGER MECHANISM

Figure 3 is a perspective drawing of the device used to trigger the sampling system. The flame sensor-trigger device (3-4) was developed for use with barriers to suppress coal dust explosions in underground mines (5). The principal feature of the device is a dual infrared flame sensor combined with a pressure-arming element. This combination prevents false and premature triggering. The device is mounted to the rib approximately 1 m from the floor, and 61 m from the face in the LLEM D drift.

A schematic of the basic circuit is shown in figure 4. During explosions the pioneer wave activates the pressure switch, energizing relay A to supply power to the dual infrared sensors. Once fired, relay A remains energized for a minimum of 3 s, the time being controlled by the capacitance of capacitor C1 and the inductance and resistance of relay A. This keeps the device armed for sufficient time for the flame to reach the trigger device. The view field of one of the flame sensors across the main entry is displaced from the other by a horizontal angle of 25°. Each sensor must detect radiation simultaneously to energize the firing of relay B.

Once fired, the output pulse of relay B activates relay C, allowing the preset time-delay relays to control the signal to the high-speed, direct-solenoid actuated valves, which control the sequential sampling at the station located 30 m downstream. A typical sample time is on the order of 100 ms, which is quite adequate for filling the collection tube (1). A detailed description of the trigger device can be found in reference 3. The system allows sampling of the leading edge of the flame where the combustion process is most intense and critical for further flame propagation.

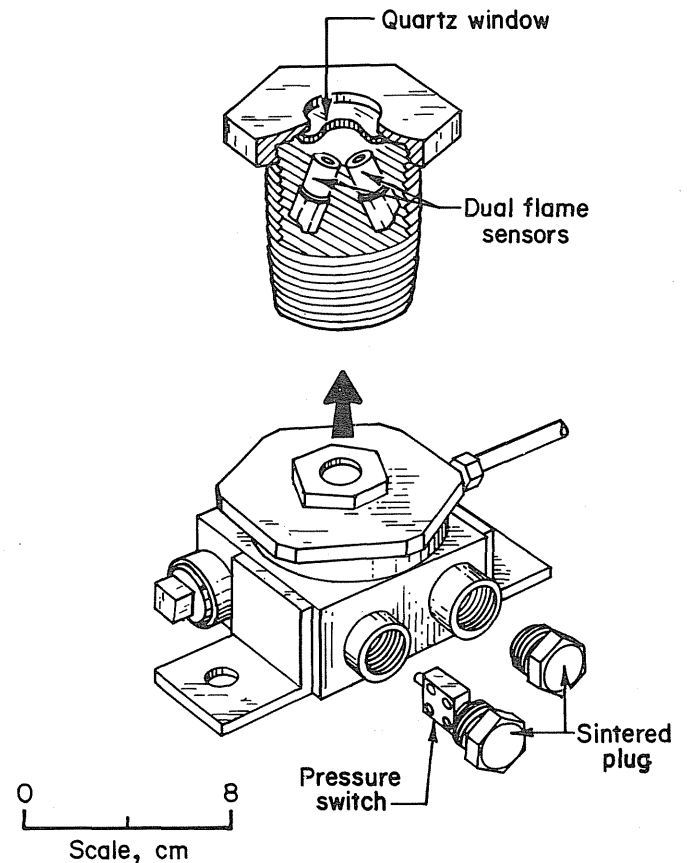
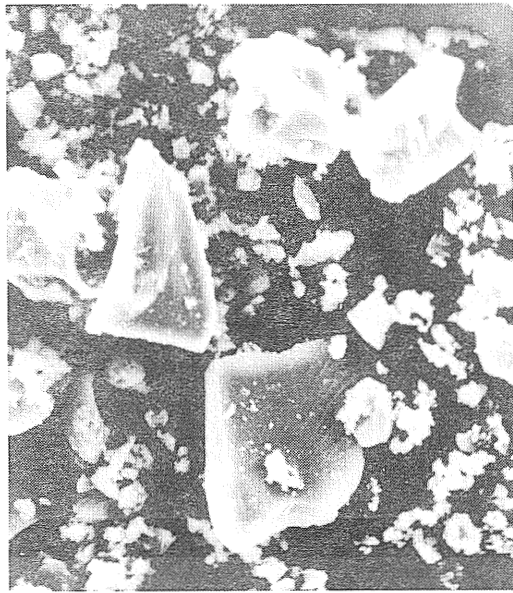
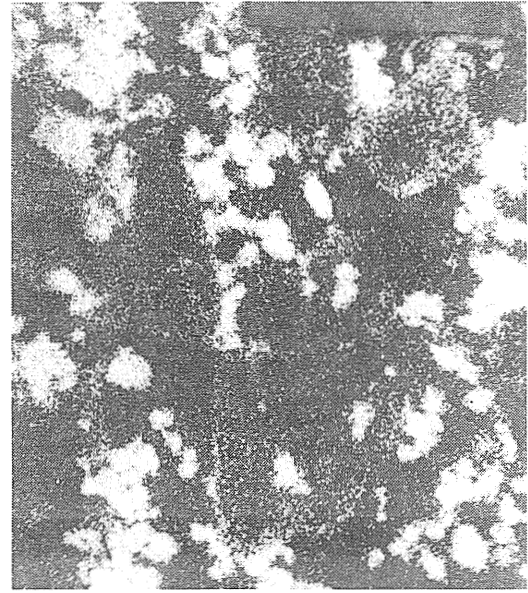


Figure 3. - Perspective view of triggering mechanism.



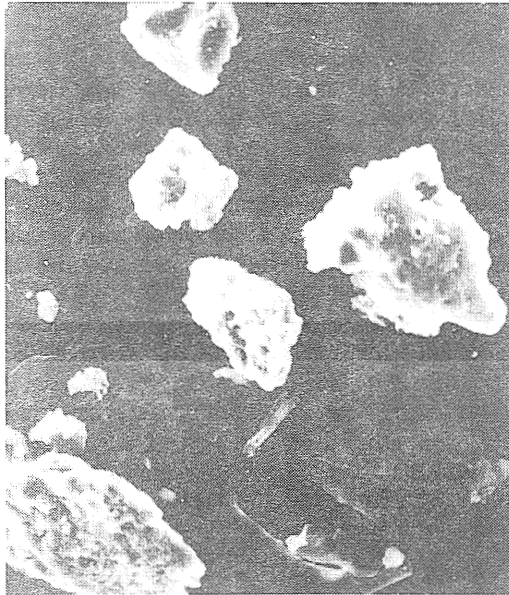
*A* Unburned

0 50  
Scale,  $\mu\text{m}$



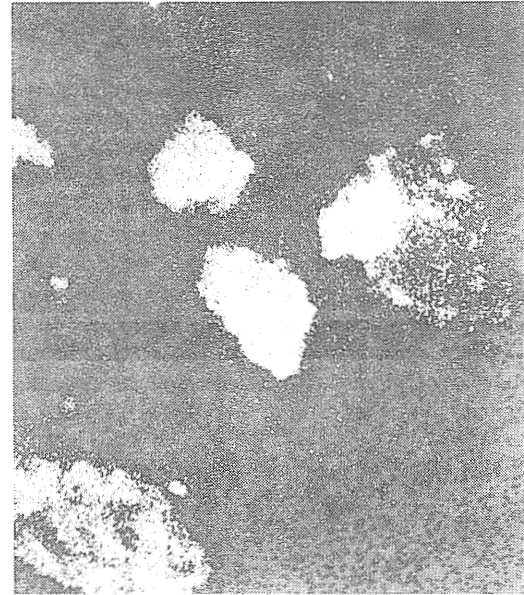
*C* X-ray map, rock dust

0 50  
Scale,  $\mu\text{m}$



*B* Burned

0 50  
Scale,  $\mu\text{m}$



*D* X-ray map, rock dust

0 50  
Scale,  $\mu\text{m}$

Figure 5. - Typical SEM photomicrographs of burned and unburned Pittsburgh coal and 65% rock dust particles, X-ray maps made using calcium line.

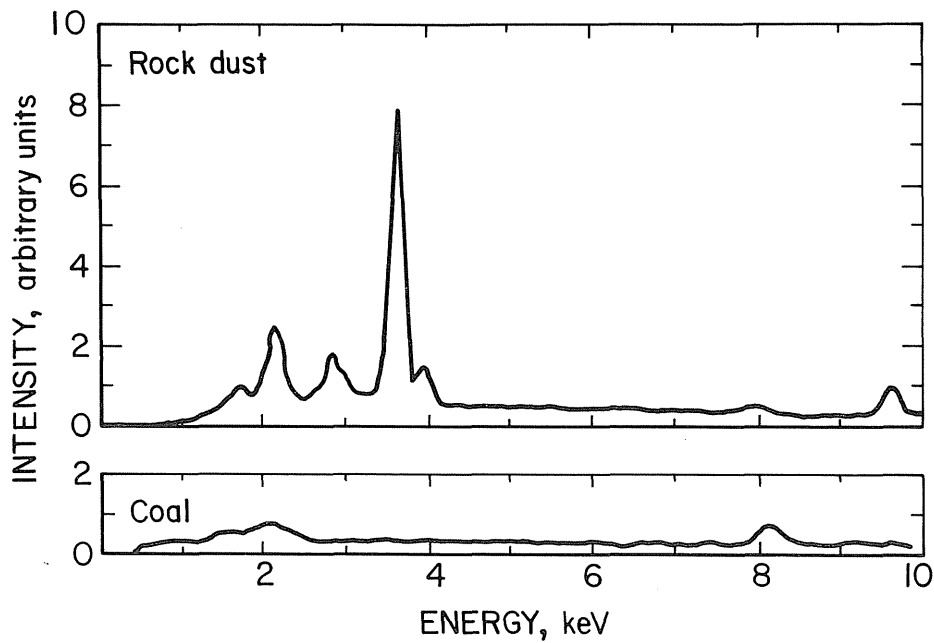


Figure 6. - X-ray spectra of Pittsburgh coal and rock dusts.

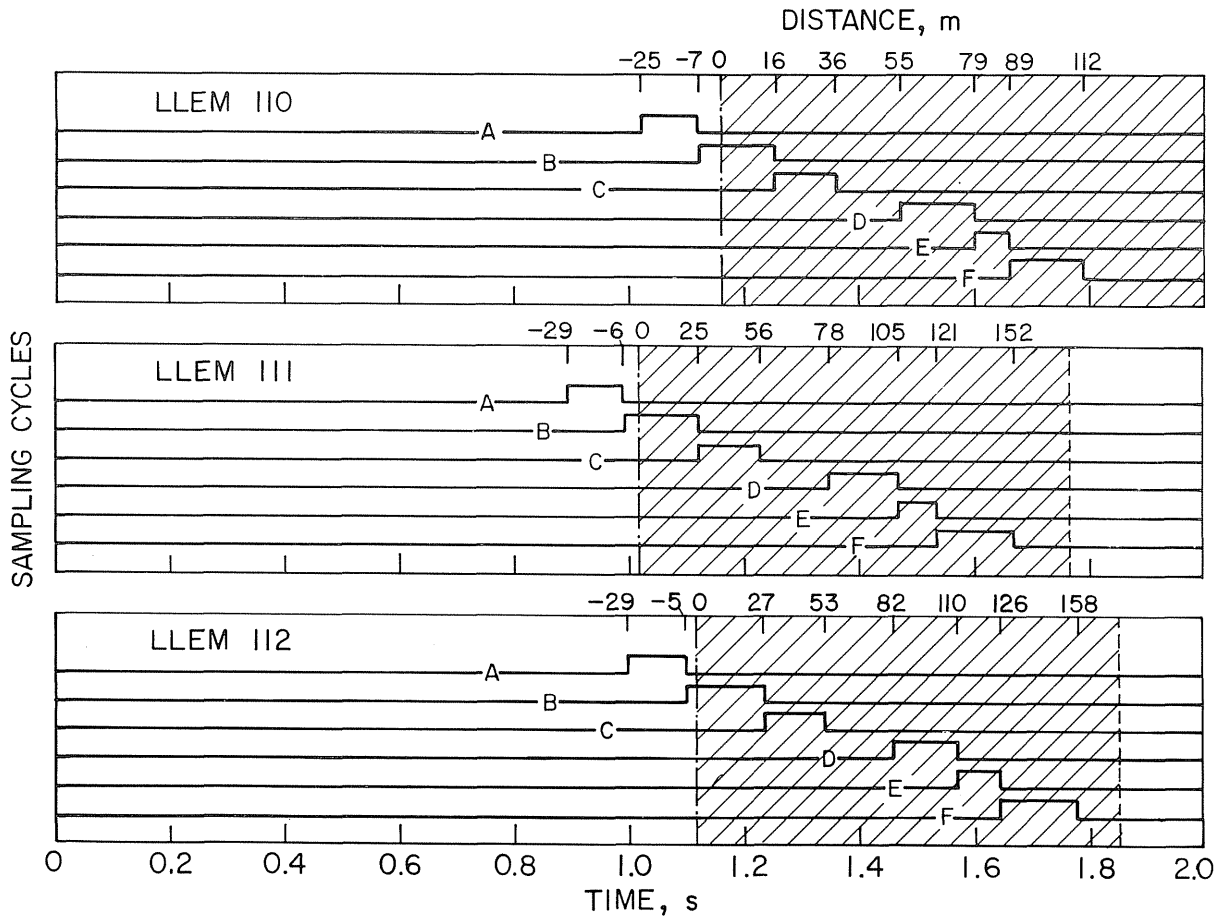


Figure 7. - Illustration of typical sampling cycle with respect to flame arrival and to trailing edge of flame for three Lake Lynn experiments.

### LAKE LYNN EXPERIMENTAL MINE

The studies were conducted with the sampling system installed in the D drift of the Lake Lynn Laboratory experimental mine. The Lake Lynn Laboratory, formerly a limestone mine (7), is now a multipurpose mining research laboratory operated by the Bureau. The laboratory underground layout, shown in figure 8, allows full-scale research of explosion propagation and

suppression as encountered in modern U.S. coal mining. The new entries dimensions range from 1.8 to 2.3 m high by 5.3 to 6.7 m wide. The average dimensions are 2.1 and 5.8 m for an average cross-sectional area of 12 m<sup>2</sup>. A plan view of the face area in D drift is given in figure 9 and shows the configuration for a single entry dust explosion.

#### LAKE LYNN LABORATORY

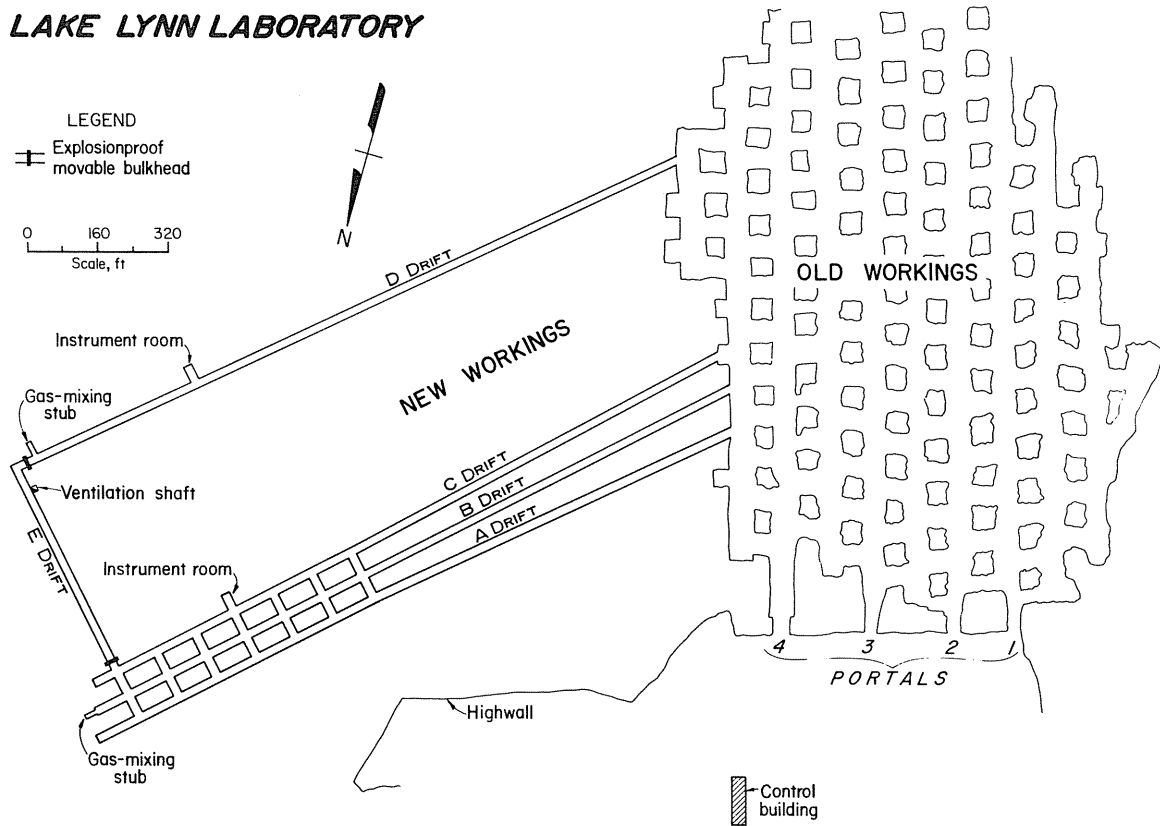


Figure 8. - Plan view of Lake Lynn underground mine.

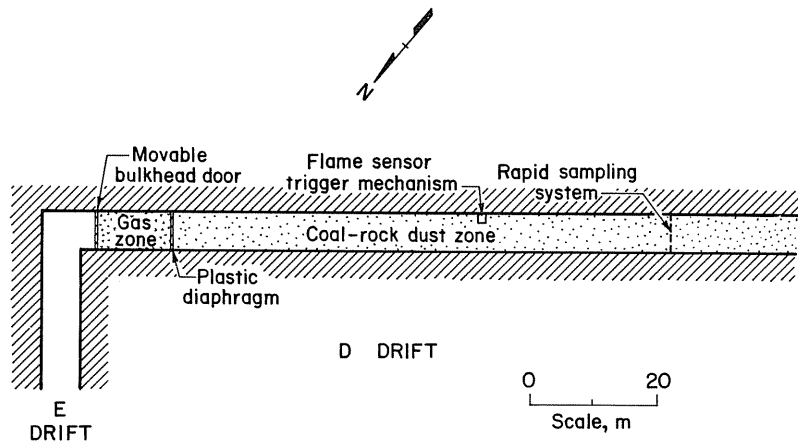


Figure 9. - Plan view of face area in D drift showing configuration of nominal dust loading for a single entry.

A flammable mixture of methane and air, typically 10%  $\text{CH}_4$ , is introduced in the gas zone, whose length varies from 3.7 to 12 m to provide weak to strong ignitions, respectively. A mixture of rock dust and/or pulverized (80% minus 200 mesh) Pittsburgh seam coal (PPC) is spread on the floor and on shelves in the dust zone (typically 107 m) to provide a PPC dust concentration near  $200 \text{ g/m}^3$ , if the dust were uniformly dispersed throughout the dust zone volume by the methane-air explosion.

A flammable dust mixture is dispersed and ignited by the methane-air explosion, causing rapid flame propagation down the entry. Instrumentation to monitor pressure

development, dust concentration (8-9), and flame arrival times is provided at 11 stations along 229 m of the entry, starting at the bulkhead. A detailed description of the physical arrangement and instrumentation for dust explosion studies at the Lake Lynn experimental mine are given in references 10 and 11.

The series of explosions involving coal dust mixtures that is described here (LLEM 110, 111, 112) consisted of a 107-m dust zone containing 60% or 65% pulverized limestone with PPC, at a nominal concentration of  $200 \text{ g/m}^3$ , that was ignited by a 12-m gas zone consisting of a 10.3% methane-air mixture. Figure 10 is a wave

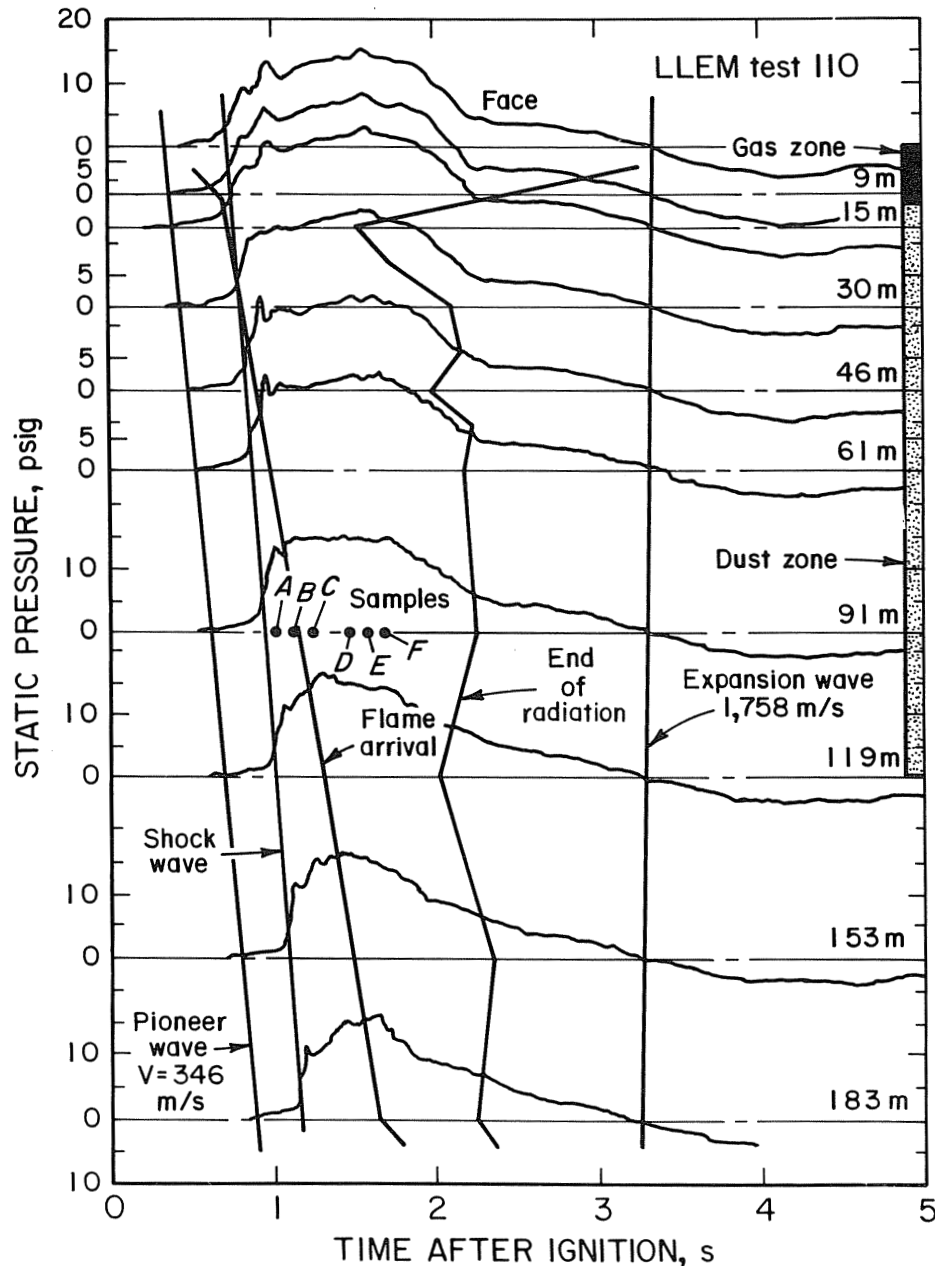


Figure 10. - Wave diagram of single-entry coal dust 65% rock dust explosion LLEM test 110, D drift.

diagram of one such explosion (LLEM 110). It plots the change in static pressure with time at the various stations, and includes data on sampling times as well as flame arrival and decay.

The complete sampling system setup at one of the monitoring stations consists of six sampling devices mounted on two vertical stands. The two stands were mounted vertically 91 m from the face and secured to the mine floor and roof by bolts. Figure 11 is a cross-sectional view of D drift and shows the sampling system and the relay control package. The roof shelves or dust trays are in place, as are the dust barrels. The latter are removed once their contents are spread out on the floor and shelves of the dust zone.

### LLEM TEST 110

Particle collection data of the sampling system in this explosion, which featured a dust mixture containing 65% rock dust, are presented in table 1. The starting time,  $t_s$ , of each sampling device is measured with respect to the initiation of the explosion. The total sample time is  $\Delta t$ ,

and  $t_f$  is the duration of sampling of the burned gases behind the flame front. The residue,  $m_C$ , collected for each sample was weighed using a microbalance and then microscopically analyzed. Sample A, taken just prior to flame arrival, shows the largest amount collected. Sample B was drawn before and during the flame, whereas C through F were taken entirely within the flame. The mass sampling rate was taken as the ordinary average over the injection interval. Actually, the collection rate decays exponentially with time, with most of the sample being collected within the first 30 ms (see figure 3 in reference 1). Samples collected from within the flame sampled a 10- to 23-m flame length, depending on the speed of flame propagation. Generally, as the flame progressed down the entry, the linear rate of residue collected decreased with increasing distance behind the flame front.

The photo micrographs of the unburned and burned dust particles from the explosion (LLEM 110) are shown in figure 12. After the explosion, the particles are noticeably larger than before the explosion. They exhibit rounded smooth surfaces in contrast to angular and sharp edges of the particles before the explosion. Many of the

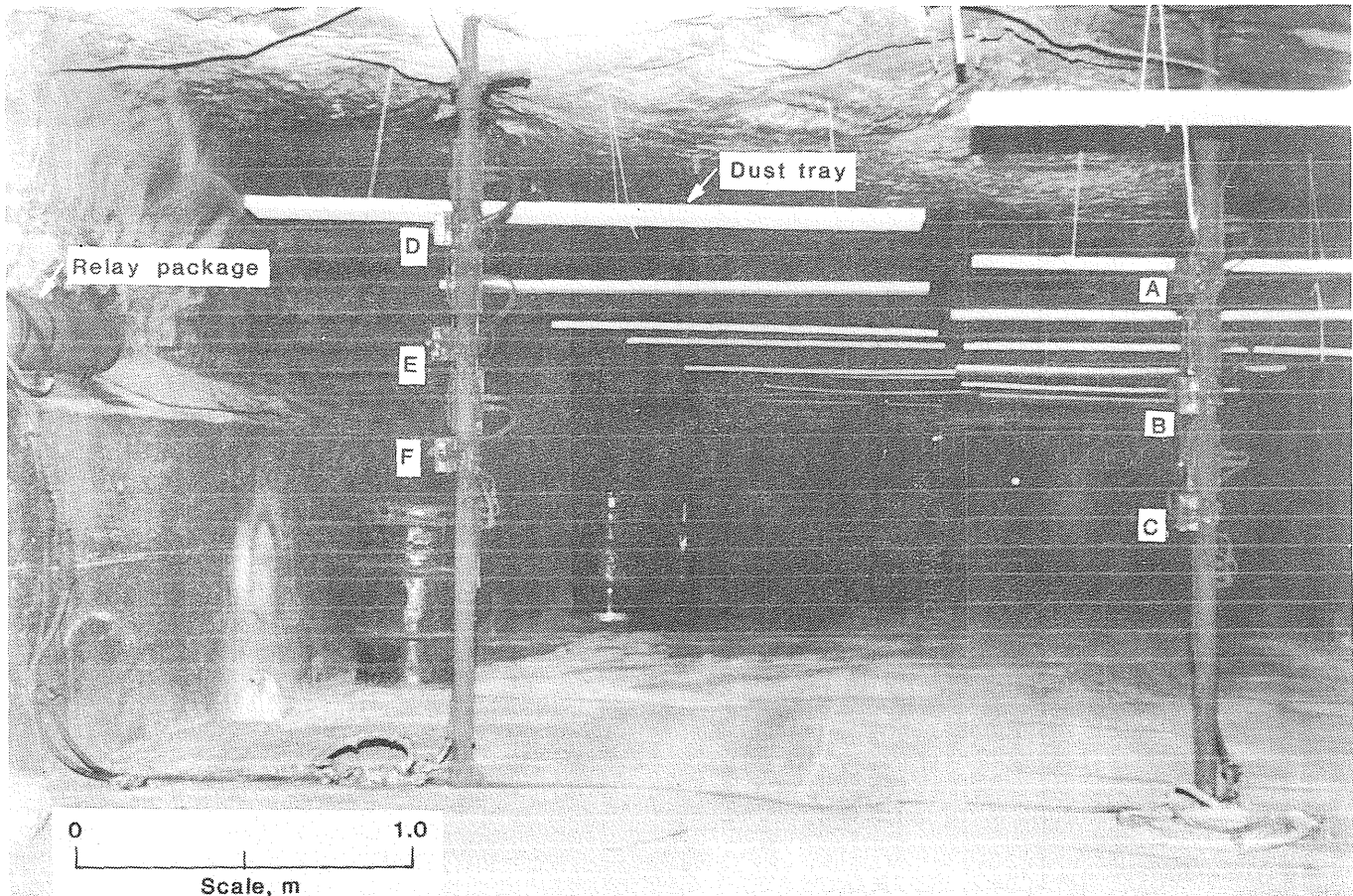


Figure 11. - Complete sampling system installed in D drift.

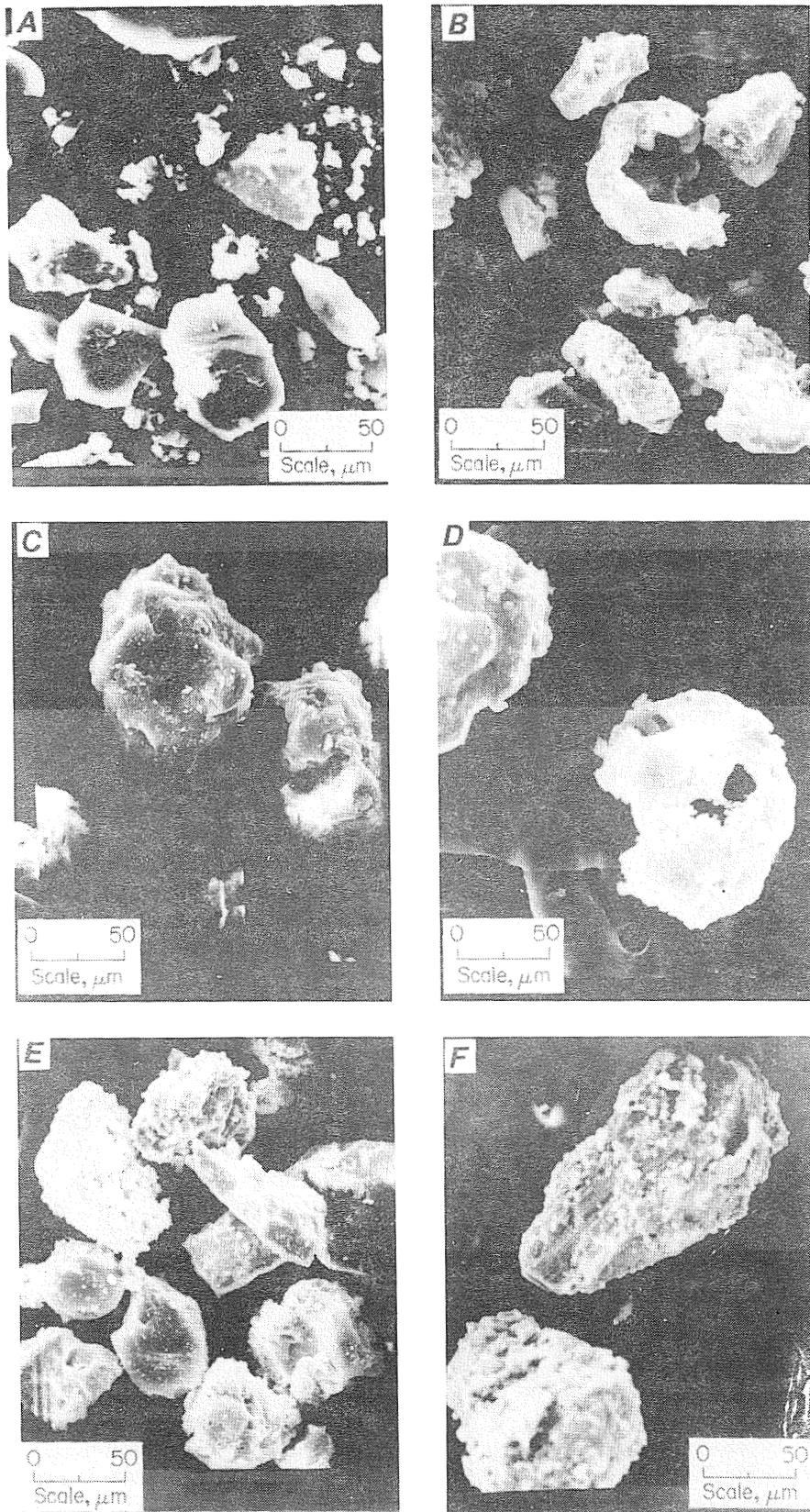


Figure 12. - Photomicrographs of dust collected with sampling device during LLEM 110 explosion test in D drift.



**TABLE 1. - Performance of sampling system**  
(LLEM test 110, flame arrival 1.161 s)

Station	Sample start ( $t_s$ ), ms	Sample interval Duration ( $\Delta t$ ), ms	In flame ( $t_f$ ), ms	Mass residue collected ( $m_c$ ), mg	Collection rate ( $r$ ), mg/ms	Flame length sample ( $l_s$ ), m
A ...	1,021	99	0	50.85	0.51	0
B ...	1,120	130	89	15.43	.12	15.9
C ...	1,250	110	110	8.58	.08	19.7
D ...	1,470	130	130	7.91	.06	23.3
E ...	1,600	60	60	4.41	.07	10.7
F ...	1,660	130	130	6.26	.05	23.3

particles in the explosion show blowholes and bubbly masses, and some have formed cenospheres. This is due to rapid heating of the particles that leads to outgassing of volatiles, which are then burned. This outgassing causes the softened coal particle to swell and eventually leads to the formation of blowholes of various sizes.

Sample A, collected just before flame arrival, shows no evidence of burned or charred particles (fig. 12A). The composition of the corresponding gas sampled is that of background air mixed with 0.6% pyrolysis gases (table 1-2). The contribution of combustion products from the methane-air zone to this sample is thus minimal, as will be explained in the "Gas Analyses" section. Sample B, shown in figure 12B, was collected primarily before flame arrival but with continued sampling into the flame front. A microscopic evaluation of this dust at several view fields indicates that about 10% of the particles are melted or charred, and several particles even have blowholes. The largest charred coal particle measures 150 to 200  $\mu\text{m}$  in diameter. The corresponding gas sample is a mixture of air and pyrolysis-combustion gases.

The remaining photo micrographs of the dust residues, samples C through F, (figs. 12C-12F) show that practically every particle has reacted. The angular features are totally absent, indicating that the particles have undergone considerable heating and devolatilization. The largest particle collected from this test measured 400  $\mu\text{m}$  in diameter. Furthermore, agglomeration is quite evident.

In a few cases, the original particles have agglomerated to huge masses with diameters of the orders of 1,000  $\mu\text{m}$ . These large agglomerates were most likely formed in the collection tube, while the particles were still plastic. The corresponding gas samples consist almost entirely of combustion-pyrolysis products as shown in table 2. Residual oxygen was only 0.6% and there was 17%  $\text{CO}_2$  as well as 5% coal pyrolysis products.

### LLEM TEST 111

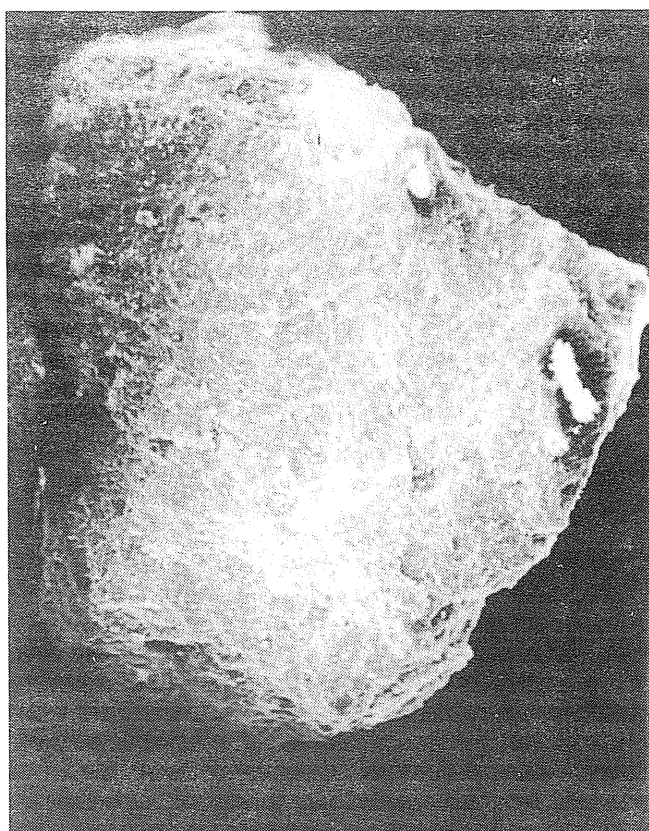
Microscopic evaluations and gas analyses were made of a similar test of a 60% limestone-PPC dust mixture (LLEM 111). SEM results indicate that 10% of the dust particles collected at station A, just before the apparent flame arrival, are melted. The largest unburned coal particle measures 200 to 225  $\mu\text{m}$  in diameter and the diameter of the largest coal particle that exhibits signs of charring is 125  $\mu\text{m}$ . The largest rock dust particle observed is in the 200- to 325- $\mu\text{m}$  range. The associated gas sample is predominantly background air with only 0.5% pyrolysis-combustion products.

The sample taken at station B just before the flame front arrival and continuing afterwards, indicates that 90% of the coal is melted or charred. In addition, large agglomerates are formed and some of the coal particles show evidence of blowholes and large areas of molten bitumen. The associated gas sample and those taken at stations C through D contain predominantly combustion-pyrolysis products with only 0.6% residual oxygen. In the residue collected entirely in the flame zone (stations C-D), there are several large (1,100  $\mu\text{m}$ ) mineral particles, as shown in figure 13, but very few coal particles. The largest burned coal particles ranged from 300 to 550  $\mu\text{m}$  in diameter. The sampling of these large particles indicate that the sampling system is capable of collecting dust particles over a wide range of sizes. The greater turbulence associated with this test may be responsible for the earlier and more intensive particle pyrolysis previously noted.

**TABLE 2. - Actual burned gas compositions from LLEM tests 110, 111, 112, with corresponding flame arrival times of 1.161 s, 1.021 s, and 1.119 s, respectively**

LLEM test	Sampling		Vol %							ppm				
	Start ( $t_s$ ), ms	In flame ( $t_f$ ), ms	$\text{N}_2$	$\text{A}_r$	$\text{O}_2$	$\text{CO}_2$	CO	$\text{H}_2$	$\text{CH}_4$	$\text{C}_2\text{H}_2$	$\text{C}_2\text{H}_4$	$\text{C}_2\text{H}_6$	$\text{C}_3\text{H}_6$	$\text{C}_3\text{H}_8$
110 A <sup>1</sup> ...	1,021	0	77.87	0.93	20.60	0.45	0.614	0.025	0.007	22	18	5	2	0
110 B ...	1,120	89	77.76	.93	5.41	11.38	3.33	.930	.154	372	277	74	39	10
110 C ...	1,250	110	75.67	.91	.74	15.83	4.96	1.490	.201	740	533	27	40	1
110 D ...	1,470	130	75.01	.90	.48	18.99	3.08	1.290	.052	339	32	3	2	0
110 E ...	1,600	60	76.31	.91	.78	17.02	3.98	.832	.054	215	123	12	16	1
110 F ...	1,660	130	77.36	.93	.33	16.88	3.80	.675	.006	12	23	6	5	0
111 A <sup>1</sup> ...	897	0	78.15	.94	20.10	.54	.106	.330	.017	31	26	8	3	1
111 B ...	996	105	74.12	.89	.65	15.19	6.69	1.960	.292	719	287	11	12	0
111 C ...	1,127	116	72.79	.87	.28	13.18	9.40	2.950	.375	622	392	12	10	0
111 D ...	1,354	116	74.62	.89	9.12	8.66	4.75	1.650	.198	281	201	6	5	0
111 F ...	1,536	130	73.32	.88	2.21	12.68	7.90	2.580	.277	399	320	8	8	0
112 B ...	1,101	115	76.10	.91	1.49	14.89	5.07	1.280	.115	898	582	22	31	1
112 C ...	1,234	115	73.27	.88	1.44	12.80	8.27	2.610	.499	841	634	48	36	4
112 F ...	1,642	30	73.37	.88	5.87	10.80	6.58	1.940	.417	579	451	8	8	0

<sup>1</sup>Samples contained background air and trace burned gas.

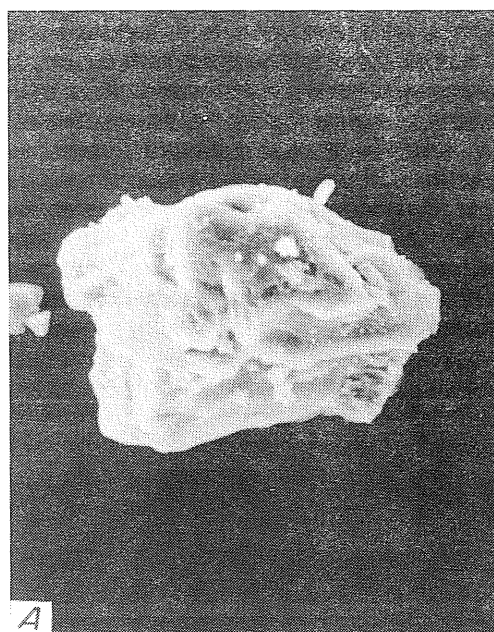


0 400  
Scale,  $\mu\text{m}$

Figure 13. - Photomicrograph of large residue collected with sampling system.

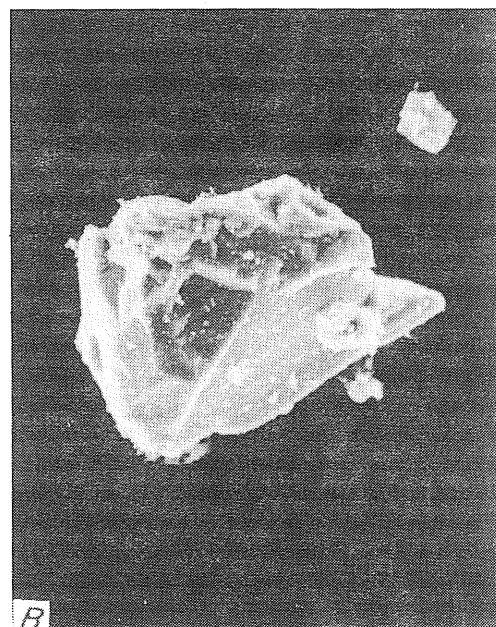
#### LLEM TEST 112

The following photomicrographs (figs. 14-15) reveal what happens when the devolatilization process of a coal particle is interrupted. Normally, as the explosion propagates down the entry, the pyrolysis process of the coal continues to near completion and the reacting gases continue to supply fuel to the fire ball. When particles are "grabbed" from the explosion environment and collected, their devolatilization process is quenched. The two partially devolatilized coal particles shown in figure 14 were collected just prior to (fig. 14A) and just after (fig. 14B) flame arrival in LLEM test 112. In figure 14A, notice the charred residue or liquid bitumen in the central portion of the particle, clearly showing the unreacted coal residue with its angular features near the bottom. This bubbly mass or char is more pronounced in the coal particle collected during the initial flame passage (fig. 14B). Again the char layer is quite evident in the top portion of



Partially burned

0 50  
Scale,  $\mu\text{m}$



Partially burned

0 50  
Scale,  $\mu\text{m}$

Figure 14. - Photomicrographs of partially devolatilized coal particles, sampled before and during the explosion.

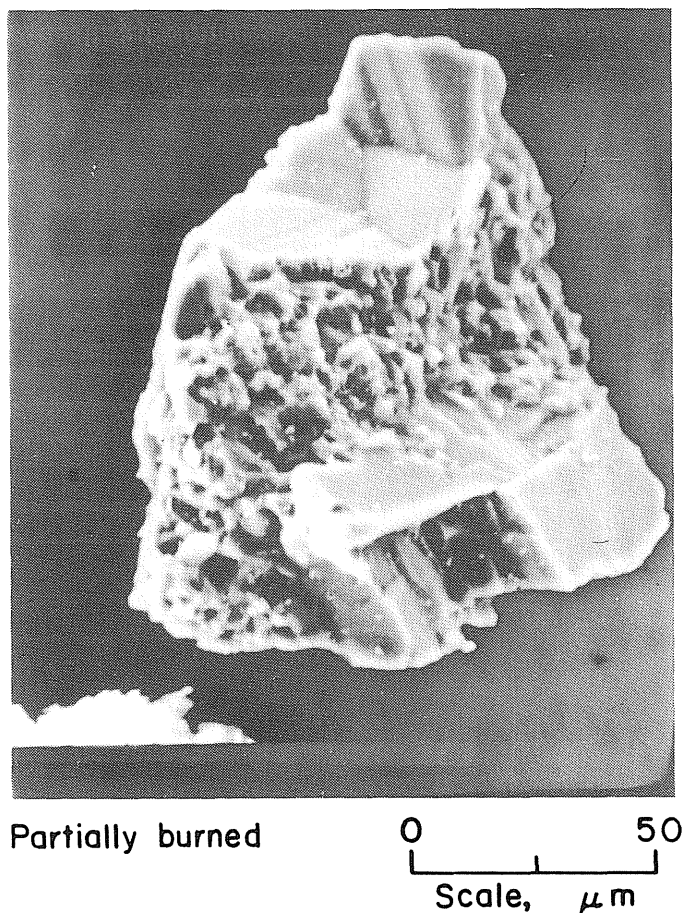


Figure 15. - Photomicrograph of partially devolatilized coal particle.

that particle. Figure 15 shows another partially devolatilized coal particle. Here the molten bitumen is centrally located and the ends expose the angular features of the unreacted coal.

The partially devolatilized coal particles from LLEM test 112 that appear to precede the flame front support the nonisothermal, flux driven volatilization model of Hertzberg (12), whose unidirectional laser heated solids

show similar structure. Those particles were about two-thirds devolatilized after an exposure to a laser flux of  $100 \text{ W/cm}^2$  for 1 s. The net absorbed flux in the laser experiment ( $75 \text{ W/cm}^2$ ) is not much higher than the calculated flux for a stoichiometric hydrocarbon flame. The similarities of the particle structures are striking, and may reflect unidirectional radiative heating in advance of the flame front.

## GAS ANALYSES

Gas samples were collected both before and after flame arrival at the sampling station, as previously described. These were dried and analyzed by gas chromatography for  $\text{N}_2$ ,  $\text{Ar}$ ,  $\text{O}_2$ ,  $\text{CO}_2$ ,  $\text{CO}$ ,  $\text{H}_2$ ,  $\text{CH}_4$ ,  $\text{C}_2\text{H}_2$ ,  $\text{C}_2\text{H}_4$ ,  $\text{C}_2\text{H}_6$ ,  $\text{C}_3\text{H}_6$ ,  $\text{C}_3\text{H}_8$ ,  $\text{C}_4\text{H}_{10}$ , and  $\text{C}_5\text{H}_{12}$ . Samples collected prior to flame arrival gave an average composition that is very close to standard dry air, as shown in table 3.

This finding is not as obvious as it may seem. Consider that typically a 12-m zone from the D drift bulkhead filled with stoichiometric methane-air is ignited. If the combustion products from the resulting methane explosion are mixed with the remaining air in the 119-m zone to the

sampling station, then significant concentrations of  $\text{CO}_2$  (1.4%) from that explosion should be detected. The fact that the  $\text{CO}_2$  concentration is increased on average from the 0.03% of standard air to 0.09% indicates that longitudinal gas mixing is minimal and that the hot burned gas acts primarily as a piston, pushing the coal-dust-laden air ahead of it. Richmond and Liebman had reached the same conclusion on the basis of explosion measurements made in the experimental mine at Bruceton (13-14).

Also shown in table 3 is the average composition of the samples collected after flame arrival. These results do not include the few samples whose compositions gave evidence

TABLE 3. - Average gas composition (dry basis), percent

Sampling	N <sub>2</sub>	A <sub>r</sub>	O <sub>2</sub>	CO <sub>2</sub>	CO	H <sub>2</sub>	CH <sub>4</sub>	C <sub>2</sub> H <sub>2</sub>	C <sub>2</sub> H <sub>4</sub>	C <sub>2</sub> H <sub>6</sub>	C <sub>3</sub> H <sub>6</sub>
Before flame . . . .	78.07	0.933	20.77	0.087	0.0024	0	0.0016	0	0	0	0
$\sigma_m$ ( $\pm$ ) . . . . .	.06	.002	.10	.016	.0012	0	.0004	0	0	0	0
After flame . . . . .	74.82	.896	.51	15.95	5.59	1.77	.232	.043	.025	.0013	0.0014
$\sigma_m$ ( $\pm$ ) . . . . .	.37	.004	.06	.52	.47	.68	.035	.006	.005	.0003	.0003

NOTE.—The error limits are the standard deviation of the mean values,  $\sigma_m = \sigma/\sqrt{n}$

of air dilution (leaking). The average Flame zone composition consists of both coal vapors and their combustion products. The former consists of the hydrocarbon gases (CH<sub>4</sub>, C<sub>2</sub>H<sub>2</sub>, C<sub>2</sub>H<sub>4</sub>, C<sub>2</sub>H<sub>6</sub>, C<sub>3</sub>H<sub>6</sub>, etc.) as well as H<sub>2</sub> and some of the CO and CO<sub>2</sub> produced.

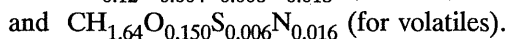
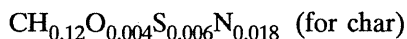
The gas compositions for the individual samples taken at the sampling stations for LLEM tests 110, 111, and 112 are shown in table 2. The large gradient in gas concentrations just within the leading edge of the flame is apparent.

## THERMODYNAMIC CALCULATIONS

The PPC used was mined at Bruceton and had the following average proximate (weight) analysis (ASTM D3173, 3174, 3175): volatiles, 37%; fixed carbon, 55%; ash, 6%; and moisture 2%. The following moisture and ash-free elemental, mass analysis has been obtained for this coal: C, 84%; H, 5.5%; O, 7.5%; S, 1.3%; and N, 1.7%, corresponding to the empirical formula, CH<sub>0.78</sub>O<sub>0.067</sub>S<sub>0.006</sub>N<sub>0.017</sub>.

The coal produces a char in the ASTM D3175 analysis for volatiles, which has the elemental analysis 95% C, 1% H, 0.5% O, 1.5% S, and 2% N. The corresponding empirical formula is CH<sub>0.13</sub>O<sub>0.005</sub>S<sub>0.006</sub>N<sub>0.014</sub>.

It is generally recognized (15) that the ASTM D3175 analysis for volatiles in bituminous coals underestimates the volatile yields under high heat flux conditions, such as in a flame front. For example, using uniform CO<sub>2</sub> laser irradiation (10.6- $\mu$ m wavelength), at flux levels of 100 to 400 W/cm<sup>2</sup>, gave volatile yields of 45% to 55% for this coal (16). Taking the true volatility as 50%  $\pm$  5% gives the following: 47.5 g C, 0.5 g H, 0.25 g O, 0.75 g S, and 1.0 g N per 50 g char, and 36.5 g C, 5 g H, 7.25 g O, 0.55 g S, and 0.7 g N per 50 g volatiles. This leads to the empirical formulas



To simplify the thermodynamic calculations, Pittsburgh coal is taken to consist of an inert carbon char (50%) and volatiles having the formula, CH<sub>1.7</sub>O<sub>0.15</sub>, in view of the uncertainties in the analysis and in the true volatility. The heat of formation of the reactants is -5,000 cal per formula

weight for the volatiles and 0 for the inert carbon. The NASA-LEWIS thermodynamic program (CEC-80) then predicts an adiabatic flame temperature at 1 atm of 1,381 K for the lean limit concentration (90 g/m<sup>3</sup>) of the coal. This flame temperature is the same as that given by a detailed model of the volatiles, tar, char, and ash produced from pyrolyzing Pittsburgh seam coal (17), as well as that of polyethylene at its limit concentration of 35 g/m<sup>3</sup>.

The addition of rock dust to the coal results in a dissipation of the combustion energy in heating the inert dust. The dissipation is stronger, however, if the CaCO<sub>3</sub> dust is allowed to decompose to gaseous CO<sub>2</sub> and a solid residue of CaO. The predicted equilibrium gas concentrations for a coal dust-rock dust mixture containing 65% CaCO<sub>3</sub> contains 16% CO<sub>2</sub> (dry basis) if the CaCO<sub>3</sub> is inert, and 24% CO<sub>2</sub> (dry basis) if CaCO<sub>3</sub> is allowed to react. The measured, average CO<sub>2</sub> concentration in the flame zone is 16%, in agreement with the inert rock dust model. The predicted rock dust concentration required to bring the flame temperature down to the 1,380-K limit is 87% for this model. Reactive CaCO<sub>3</sub>, however, requires only 75%, in agreement with measurements made in the experimental mine at Bruceton as well as in the 20-L explosion chamber (18). However, results to date at the Lake Lynn Laboratory indicate an inerting level of 80% rock dust (19). The overall results suggest that only part of the rock dust actually reaches a decomposition temperature of 1,180 K to form CO<sub>2</sub>, and not all pyrolysis products are oxidized to CO<sub>2</sub> in the presence of a limited O<sub>2</sub> concentration.

## CONCLUSIONS

Immediately prior to flame arrival, the background gas is virtually that of standard air and few particles show signs of tar, volatiles, or char formation. Gas samples in the leading edge of the flame show the large concentration changes characteristic of the flame front. Gas samples taken entirely in the flame zone consist of pyrolysis and combustion products. The particles show signs of extensive pyrolysis and charring. The correspondence between the value of the principal gases ( $N_2$ ,  $O_2$ , and  $CO_2$ ) as calculated for inert (nondecomposing)  $CaCO_3$ -coal (PPC) mixtures burning in air and the experimental value,

suggests a limited or inefficient decomposition of the rock dust. These experimental results demonstrate the utility of the high-speed gas and dust sampling system in analyzing large-scale explosions.

The system can be further upgraded by interfacing a microprocessor or computer to enhance timing capabilities and eliminate the relay control package. For example, data from a set of flame sensors upstream of the sampling system could be used by a microprocessor to calculate the expected time of flame arrival and thereby insure sampling of the flame zone or even its leading edge.

## REFERENCES

- Conti, R. S., M. Hertzberg, F. T. Duda, and K. L. Cashdollar. Rapid-Sampling System for Dusts and Gases. *Rev. Sci. Instrum.*, v. 54, 1983, pp. 104-108.
- Conti, R. S., K. L. Cashdollar, M. Hertzberg, and I. Liebman. Thermal and Electrical Ignitability of Dust Clouds. BuMines RI 8798, 1983, 40 pp.
- Liebman, I., F. Duda, and R. S. Conti. Sensor Trigger Device for Explosion Barrier. *Rev. Sci. Instrum.*, v. 50, 1979, pp. 1441-1444.
- Liebman, I., F. Duda, and R. S. Conti. Sensor Trigger Device for Explosion Barrier. U.S. Pat. 4,173,140, Nov. 6, 1979.
- Lieman, I., J. K. Richmond, R. Pro, R. S. Conti, and J. Corry. Triggered Barriers for the Suppression of Coal Dust Explosions. BuMines RI 8389, 1979, 24 pp.
- Ng, D. L., K. L. Cashdollar, M. Hertzberg, and C. P. Lazzara. Electron Microscopy Studies of Explosion and Fire Residues. BuMines IC 8936, 1983, 63 pp.
- Mattes, R. H., A. Bacho, and L. V. Wade. Lake Lynn Laboratory: Construction, Physical Description, and Capability. BuMines IC 8911, 1983, 40 pp.
- Conti, R. S., K. L. Cashdollar, and I. Liebman. Improved Optical Probe for Monitoring Dust Explosions. *Rev. Sci. Instrum.*, v. 53, 1982, pp. 311-313.
- Cashdollar, K. L., I. Liebman, and R. S. Conti. Three Bureau of Mines Optical Dust Probes. BuMines RI 8542, 1981, 26 pp.
- Sapko, M. J., E. S. Weiss, and R. W. Watson. Size Scaling of Gas Explosions: Bruceton Experimental Mine Versus the Lake Lynn Mine. BuMines RI 9136, 1987, 23 pp.
- M. J. Sapko, N. Greninger, and E. S. Weiss. Water Barrier Performance in a Wide Mine Entry. To be presented at Third (International) Colloquium on Dust Explosions (Szczyrk, Poland), Oct. 1988.
- Hertzberg, M., I. A. Zlochower, R. S. Conti, and K. L. Cashdollar. Thermokinetic Transport Control and Structural Microscopic Realities in Coal and Polymer Pyrolysis Explosions. Paper in Proceedings, ACS Fuel Division Symposium (New Orleans, LA, Aug-Sept. 1987). ACS, 1988, pp. 24-41.
- Richmond, J. K., and I. Liebman. A physical Description of Coal Mine Explosions. Paper in Fifteenth Symposium (International) on Combustion (Tokyo, Japan). Combustion Inst., Pittsburgh, PA, 1975, pp. 115-126.
- Richmond, J. K., I. Liebman, A. E. Bruszak, and L. F. Miller. A Physical Description of Coal Mine Explosions. Part II. Paper in Seventeenth Symposium (International) on Combustion (Leeds, England). Combustion Inst., Pittsburgh, PA, 1979, pp. 1257-1268.
- Howard, J. B. Fundamentals of Coal Pyrolysis and Hydrolysis. Ch. 12 in Chemistry of Coal Utilization, Vol. 2, ed. by M. A. Elliott. Wiley, 1981, pp. 665-784.
- Hertzberg, M., and D. Ng. A Microscopic and Kinetic Study of Coal Particle Devolatilization in a Laser Beam. Paper in Fundamentals of Physical Chemistry of Pulverized Coal Combustion, ed. by J. Lahaye and G. Prado, NATO ASI Series E, No. 137. Martinus Nijhoff, 1987, p. 110.
- Hertzberg, M., I. A. Zlochower, and K. L. Cashdollar. Volatility Model for Coal Dust Flame Propagation and Extinguishment. Paper in the Twenty-first Symposium (International) on Combustion (Munich, Federal Republic of Germany, Aug. 1986). Combustion Inst., Pittsburgh, PA, 1986, pp. 325-333.
- Cashdollar, K. L., and M. Hertzberg. 20-L Explosibility Test Chamber for Dusts and Gases. *Rev. Sci. Instrum.*, v. 56, 1985, pp. 596-602.
- Cashdollar, K. L., M. J. Sapko, E. S. Weiss, and M. Hertzberg. Laboratory and Mine Dust Explosions Research at the Bureau of Mines. Sec. in Industrial Dust Explosions, ASTM STP 958. ASTM, 1987, pp. 107-118.

**APPENDIX.—LIST OF SYMBOLS**

$C_1$	capacitance, micofarads	$r$	collection rate
$t_s$	sample start	$l_s$	length of flame sampled
$\Delta t$	sample interval, duration	$\sigma_m$	standard deviation of the mean ( $\sigma/\sqrt{n}$ )
$t_f$	sample interval, in flame	%	percent
$m_c$	mass residue collected		

U.S. Department of the Interior  
Bureau of Mines--Prod. and Distr.  
Cochrans Mill Road  
P.O. Box 18070  
Pittsburgh, PA 15236

AN EQUAL OPPORTUNITY EMPLOYER

-----  
**OFFICIAL BUSINESS**  
PENALTY FOR PRIVATE USE--\$300

We do not wish to receive this material. Please remove us from your mailing list.

Our address has changed. Please correct as indicated.